The Extremely Active 2017 North Atlantic Hurricane Season

PHILIP J. KLOTZBACH[a]

Department of Atmospheric Science, Colorado State University, Fort Collins, Colorado

CARL J. SCHRECK III[a]

Cooperative Institute for Climate and Satellites, North Carolina State University, Asheville, North Carolina

JENNIFER M. COLLINS

School of Geosciences, University of South Florida, Tampa, Florida

MICHAEL M. BELL

Department of Atmospheric Science, Colorado State University, Fort Collins, Colorado

ERIC S. BLAKE

NOAA/National Hurricane Center, Miami, Florida

DAVID ROACHE

School of Geosciences, University of South Florida, Tampa, Florida

(Manuscript received 2 March 2018, in final form 15 August 2018)

ABSTRACT

The 2017 North Atlantic hurricane season was extremely active, with 17 named storms (1981–2010 median is 12.0), 10 hurricanes (median is 6.5), 6 major hurricanes (median is 2.0), and 245% of median accumulated cyclone energy (ACE) occurring. September 2017 generated more Atlantic named storm days, hurricane days, major hurricane days, and ACE than any other calendar month on record. The season was destructive, with Harvey and Irma devastating portions of the continental United States, while Irma and Maria brought catastrophic damage to Puerto Rico, Cuba, and many other Caribbean islands. Seasonal forecasts increased from calling for a slightly below-normal season in April to an above-normal season in August as large-scale environmental conditions became more favorable for an active hurricane season. During that time, the tropical Atlantic warmed anomalously while a potential El Niño decayed in the Pacific. Anomalously high SSTs prevailed across the tropical Atlantic, and vertical wind shear was anomalously weak, especially in the central tropical Atlantic, from late August to late September when several major hurricanes formed. Late-season hurricane activity was likely reduced by a convectively suppressed phase of the Madden–Julian oscillation. The large-scale steering flow was different from the average over the past decade with a strong subtropical high guiding hurricanes farther west across the Atlantic. The anomalously high tropical Atlantic SSTs and low vertical wind shear were comparable to other very active seasons since 1982.

1. Introduction

The 2017 Atlantic hurricane season was one of the most active on record, with 17 named storms (1981–2010 median is 12.0; Schreck et al. 2014), 10 hurricanes (median is 6.5), and 6 major hurricanes [category 3+ on the Saffir–Simpson hurricane wind scale; ≥ 96 kt (1 kt $\approx$ 0.5144 m s^{-1}); median is 2.0; Simpson 1974]. Integrated metrics such as major hurricane days and accumulated cyclone energy (ACE; Bell et al. 2000) also ranked in the top 10 busiest seasons when compared with the historical record since 1851 (e.g., HURDAT2; Landsea and Franklin 2013), with the Atlantic experiencing the

[a] Philip J. Klotzbach and Carl J. Schreck III are co-lead authors.

Corresponding author: Philip J. Klotzbach, philk@atmos.colostate.edu

DOI: 10.1175/MWR-D-18-0078.1

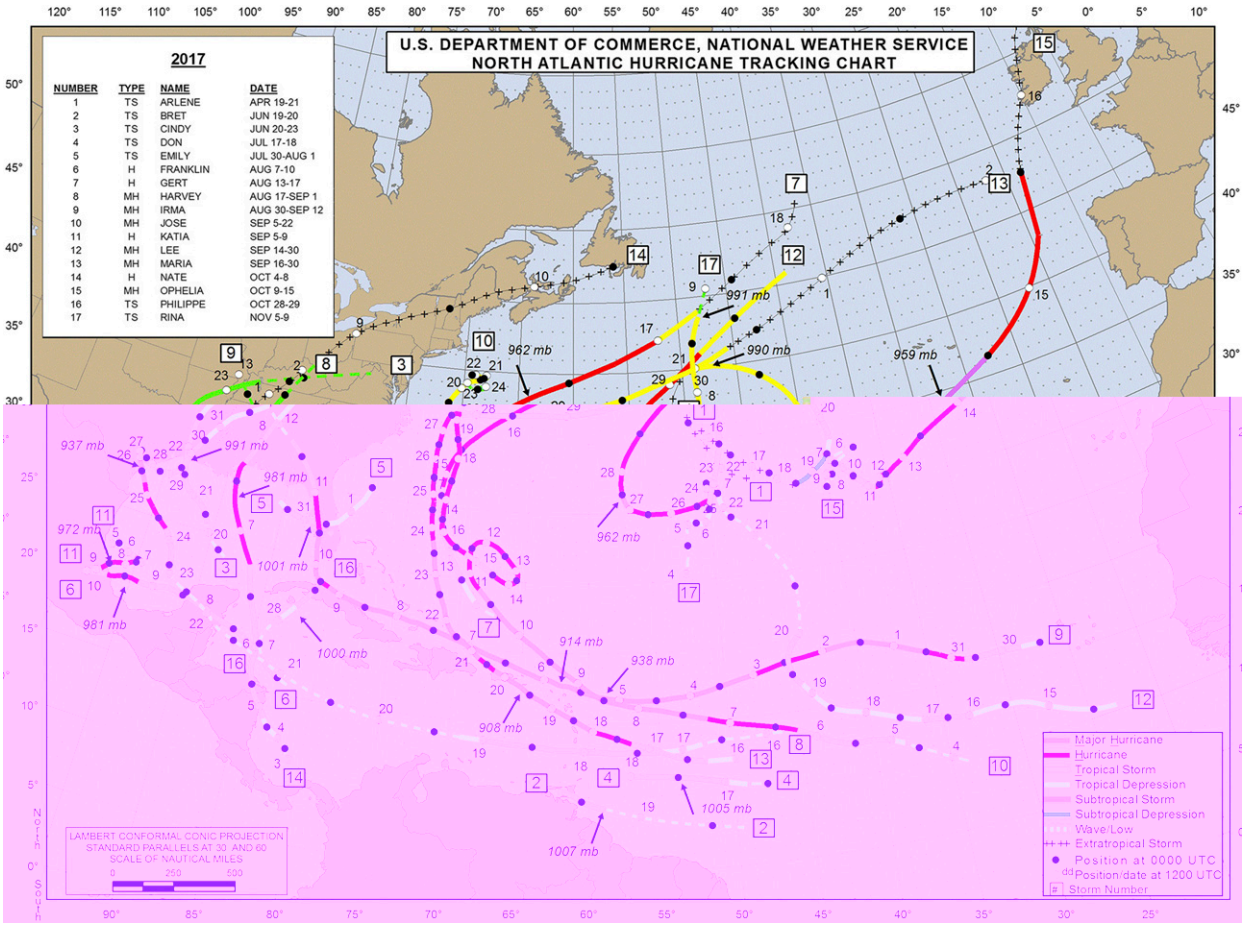

FIG. 1. Tracks of all Atlantic named storms in 2017. Figure courtesy of the National Hurricane Center (https://www.nhc.noaa.gov/data/tracks/tracks-at-2017.png).

third-most major hurricane days since 1950. The 2017 Atlantic hurricane season also generated over $260 billion (U.S. dollars) in total economic damage according to the National Centers for Environmental Information (NCEI; https://www.ncdc.noaa.gov/billions/events/US/1980-2017), rivaling 2005 as one of the most damaging seasons on record.

What set 2017 apart from most other active seasons was its extremely active September. This month set aggregate calendar month records for the Atlantic basin for named storm days, hurricane days, major hurricane days, and ACE. The Atlantic also generated more ACE in September 2017 than any calendar month on record in any global tropical cyclone (TC) basin, using boundaries defined by Klotzbach (2014). These records are not coincidences of the calendar, as the period from 31 August to 29 September 2017 generated the most Atlantic ACE in a 30-day period in the historical record (section 6).

The season was especially notable for four hurricanes (Harvey, Irma, Maria, and Nate), which were retired by the WMO following the season. Several of the TCs that formed in 2017 had long westward tracks, which caused them to impact multiple landmasses (Fig. 1). The 2017 season ended the 11-yr continental U.S. major hurricane landfall drought when Harvey made landfall northeast of Corpus Christi, Texas (Hall and Hereid 2015; Hart et al. 2016; Truchelut and Staehling 2017). In fact, it was the first year on record that the continental United States had two category 4 hurricanes make landfall (Harvey and Irma).

The remainder of this manuscript discusses the 2017 Atlantic hurricane season in more detail. We begin by describing data sources and methodology in section 2, then summarize 2017 Atlantic hurricane activity (section 3). We then examine preseason conditions as well as trends in these conditions and how they impacted seasonal hurricane forecasts (section 4). Environmental conditions during the peak of the Atlantic hurricane season from August through October are then examined (section 5), and these are compared with other

very active seasons (and 30-day periods) since 1982 in section 6. This section also includes a correlation analysis of monthly and seasonal ACE with SSTs and vertical wind shear for all hurricane seasons since 1982. Section 7 discusses how the results of this study may aid in improving future seasonal/subseasonal Atlantic hurricane outlooks and summarizes the manuscript.

2. Data and methodology

Tropical cyclone frequency, intensity, and duration data for the 2017 season and historical hurricane seasons were taken from HURDAT2 as updated on 1 May 2018 (https://www.nhc.noaa.gov/data/hurdat/hurdat2-1851-2017-050118.txt; Landsea and Franklin 2013). In addition to the maximum intensity and longevity of each TC, we considered the storm-generated ACE, as well as the ACE for the season. Bell et al. (2000) defined ACE as the sum of the squares of the maximum sustained surface wind speed (in kt) measured every 6 h for all tropical or subtropical cyclones while they have an intensity of $\geq$34 kt ($\geq$17 m s^{-1}) and are still classified as tropical or subtropical cyclones. ACE values are displayed in 10^4 kt^2 (Bell et al. 2000).

For atmospheric large-scale parameters, we use the Climate Forecast System Reanalysis (CFSR; Saha et al. 2010) from 1979 to 2011. This dataset was downloaded at 1° resolution and is available with extension to present via output from the Climate Forecast System, version 2 (Saha et al. 2014). For oceanic conditions, we use the National Oceanic and Atmospheric Administration (NOAA) Optimum Interpolation Sea Surface Temperature (OISST) dataset (Reynolds et al. 2002; Banzon et al. 2016), with data available at a daily temporal resolution and on a 0.25° global grid from November 1981 to present. Both datasets are available in near real time.

The Madden–Julian oscillation (MJO) index was calculated using the methodology described by Wheeler and Hendon (2004) and currently available from the Australian Bureau of Meteorology (http://poama.bom.gov.au/climate/mjo/graphics/rmm.74toRealtime.txt).

The Pacific Walker circulation index (Wang 2004) was calculated from the CFSR. The Pacific Walker circulation index is defined as the difference of the 500-hPa vertical velocity in the tropical western Pacific (5°S–5°N, 120°–160°E) from the tropical eastern Pacific (5°S–5°N 160°–120°W). The Pacific Walker circulation index is a useful approximation for the atmospheric response in the tropical Pacific to El Niño–Southern Oscillation (ENSO) SST forcing (Rasmusson and Carpenter 1982) along with remote forcing from other basins.

When comparing environmental conditions of 2017 with historical Atlantic hurricane seasons, we examine two different climate modes: the Atlantic meridional mode (Vimont and Kossin 2007) and ENSO. Monthly values of the Atlantic meridional mode are obtained from https://www.esrl.noaa.gov/psd/data/timeseries/monthly/AMM/ammsst.data. The raw Atlantic meridional mode index is not standardized, but we have standardized it to a 1981–2010 base period. The Niño-3.4 index (5°S–5°N, 170°–120°W; Barnston et al. 1997) is used to represent ENSO and is also calculated from a 1981–2010 base period. Monthly values were obtained from http://www.cpc.ncep.noaa.gov/data/indices/sstoi.indices.

For environmental field calculations, we define the main development region as 10°–20°N, 90°–20°W, similar to the definition used by Bell et al. (2000) and Goldenberg et al. (2001). This region encompasses the tropical Atlantic as well as the Caribbean Sea. Approximately 75% of all major hurricanes in the Atlantic basin in the satellite era (since 1966) have first become named storms in the main development region, so conditions in this region are critical for determining how active an Atlantic hurricane season is going to be.

We have removed the tropical cyclone–related circulation from all wind and steering flow calculations. Following Galarneau and Davis (2013), we defined a fixed 500-km radius around each storm location and attribute all vorticity and divergence within that radius to the storm. From the storm-related vorticity and divergence, we calculated the storm-related rotational and irrotational winds. These are each subtracted from the original winds to produce a wind field without the effect of the storm. Vertical wind shear is calculated as the vector wind difference between the 200- and 850-hPa levels.

3. Observed 2017 North Atlantic hurricane activity

a. 2017 season summary discussion

The 2017 Atlantic hurricane season was extremely active. Through late August, however, Atlantic TC activity was near its long-term ACE average (Fig. 2), despite Hurricane Harvey. Harvey was an intense hurricane, but because its time as a major hurricane was short-lived, the cyclone generated only modest ACE. September 2017, on the other hand, was the most active calendar month on record for the Atlantic for several intensity and duration metrics including named storm days, hurricane days, major hurricane days, and ACE (Fig. 2). The ACE generated in September 2017 was 3.5 standard deviations greater than the 1981–2010 average. Three hurricanes (Irma, Jose, and Maria) reached individual ACE values of greater than 40 during September. Based on satellite era data

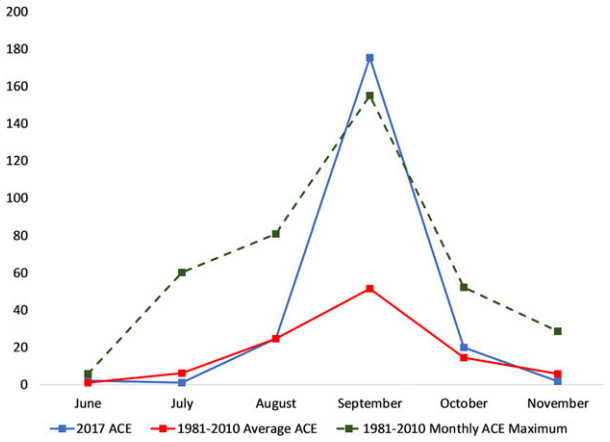

FIG. 2. Atlantic ACE by month in 2017 (blue line), compared with both the 1981–2010 average (red line) and the HURDAT2 monthly maximum (green line).

from 1966 to 2016, only 2% of all Atlantic TCs accrued an ACE of 40 or higher, and only 4 years since 1851 have ever had more than one. The 2017 Atlantic hurricane season was the first to have three. Post-September Atlantic hurricane activity returned to near-normal levels when measured by ACE (Fig. 2), likely due to wind shear generated by an amplified MJO event in October (section 5).

b. *Hurricane Harvey*

Hurricane Harvey rapidly intensified in the southern Gulf of Mexico in an environment of very high SSTs (>29.5°C) and low vertical wind shear (<10 kt; <5 m s^{-1}; Blake and Zelinsky 2018). Soon after reaching its maximum intensity of 115 kt (59 m s^{-1}), Hurricane Harvey made its initial landfall northeast of Corpus Christi, Texas, on 25 August, making it the first major hurricane landfall in the continental United States since Wilma in 2005 (Truchelut and Staehling 2017). Following its landfall, Harvey stalled due to strong high pressure to its northwest and northeast, and the TC dumped copious amounts of rain on the Houston metropolitan and Beaumont/Port Arthur areas (Emanuel 2017; Blake and Zelinsky 2018). Over the 5-day period up to and including 1 September, the National Weather Service reported that 60.58 in. (1539 mm) of rain fell in Nederland, Texas (Blake and Zelinsky 2018). This rainfall total is the record-highest storm total for any U.S. TC. Harvey also produced a widespread swath of 36+ in. (914+ mm) of rain across the Houston metropolitan area, including 37.01 in. (940 mm) at Houston Hobby Airport and 47.52 in. (1207 mm) at Jack Brooks Regional Airport in Beaumont, Texas (Blake and Zelinsky 2018). Total economic damage from Hurricane Harvey was estimated by NCEI to be $125 billion.

c. *Hurricane Irma*

Hurricane Irma had the strongest maximum sustained winds of the 2017 season, reaching a peak intensity of 155 kt (80 m s^{-1}; Cangialosi et al. 2018). In fact, Irma set records for the strongest maximum winds and lowest minimum sea level pressure (SLP; 914 hPa) for a hurricane in the Atlantic Ocean outside of the western Caribbean and the Gulf of Mexico. Irma's SLP record was broken by Maria less than 2 weeks later and only 250 km away, illustrating how conducive conditions were for hurricanes in this region. Irma made several landfalls as a category 5 hurricane in the Caribbean before becoming the first category 5 hurricane to make landfall in Cuba since 1924. Irma then made landfall in the Florida Keys as a category 4 hurricane with a minimum SLP of 931 hPa. Irma made a second landfall near Naples, Florida, as a category 3 hurricane. It generated the second-most ACE for an Atlantic hurricane in the satellite era, trailing only Ivan (2004). Irma was responsible for 44 direct fatalities across the Caribbean, Cuba, and the continental United States (Cangialosi et al. 2018), and total economic damage from the storm was estimated by NCEI to be $50 billion.

d. *Hurricane Maria*

Hurricane Maria had the lowest SLP (908 hPa) of the 2017 Atlantic hurricane season (Pasch et al. 2018). It became the first known category 5 hurricane to make landfall in Dominica and then impacted the U.S. Virgin Islands before making landfall as a category 4 hurricane in Puerto Rico. Maria was the second-strongest hurricane to strike Puerto Rico on record, behind only the Okeechobee Hurricane of 1928, known locally as the San Felipe Segundo Hurricane. Maria was responsible for ~100 direct fatalities, although indirect Puerto Rican fatalities in the month that followed the storm likely were in the hundreds (Pasch et al. 2018). Estimated total damage from NCEI for Maria was $90 billion.

e. *Hurricane Nate*

In early October, Nate formed in the western Caribbean and soon after made landfall in Nicaragua as a tropical storm (Beven and Berg 2018). Heavy rainfall from Nate caused massive flooding in Central America. After Nate emerged into the western Caribbean, it began to intensify as it rapidly moved northward across the Gulf of Mexico. Nate reached its maximum intensity of 80 kt in the northern Gulf of Mexico and weakened slightly before making landfall in Louisiana and then in Mississippi as a category 1 hurricane. A total of 45 direct fatalities were attributed to Nate, all in Central America. Total damage for Nate, as estimated by NCEI, was $800 million.

TABLE 1. Seasonal forecasts of named storms, hurricanes, major hurricanes, and ACE from CSU, NOAA, and TSR, respectively, issued in Apr, late May/early Jun, and early Aug. Observed 2017 values are also included for reference.

Forecast issue month	Apr		May/Jun			Aug			
Issuing organization	CSU	TSR	CSU	TSR	NOAA	CSU	TSR	NOAA	Observed
Named storms	11	11	14	14	11–17	16	17	14–19	17
Hurricanes	4	4	6	6	5–9	8	7	5–9	10
Major hurricanes	2	2	2	3	2–4	3	3	2–5	6
ACE	75	67	100	98	69–143	135	116	92–156	225

4. Analysis of March–July 2017 environmental conditions

a. Seasonal forecast summary

Table 1 displays publicly available seasonal forecasts from Colorado State University (CSU), NOAA, and Tropical Storm Risk (TSR) issued in 2017. A total of 20 seasonal forecast groups submitted predictions to http://www.seasonalhurricanepredictions.org in 2017, but the three forecasts displayed here are broadly representative of the larger suite of predictions. They are also three of the longest-running seasonal forecast groups and have demonstrated long-term real-time forecast skill (Klotzbach et al. 2017). Forecasts from TSR and CSU called for a slightly below-average season with their early April outlooks. By the time of the late May/early June outlooks, TSR, CSU, and NOAA all predicted a near-average season. These forecasts all increased to call for an above-average season by the time of the early August outlooks, but none of the three forecast groups anticipated as much activity as was observed (Table 1). We note that the dynamically based seasonal hurricane forecast from the Met Office (Camp et al. 2018) did call for an above-average season in mid-May and highlighted the potential for increased September TC tracks in the eastern Caribbean, but even this forecast did not predict as much activity as was observed. In the next two subsections, we highlight changes in both ENSO and tropical Atlantic SST configurations from boreal spring to summer. These conditions were not anticipated by most seasonal forecast groups and led to significant errors with seasonal forecasts issued during the boreal spring.

b. ENSO changes from March to July

La Niña events are often associated with more active Atlantic hurricane seasons. El Niño, on the other hand, tends to favor suppressed Atlantic hurricane activity. This is due to alterations in the Pacific Walker circulation. The stronger Pacific Walker circulation associated with La Niña reduces upper-level westerly winds in the Caribbean extending into the tropical Atlantic, thereby decreasing vertical wind shear in the Caribbean as well as the tropical Atlantic (Gray 1984; Landsea et al. 1999; Tartaglione et al. 2003; Lupo et al. 2008; Klotzbach 2011a; Patricola et al. 2014; Collins and Roache 2017). Increased Caribbean vertical wind shear tends to prevail in El Niño conditions.

Figure 3a displays standardized SST anomalies during March 2017. The tropical eastern Pacific was much warmer than normal in March. Many of the statistical and dynamical ENSO prediction models available in March (which were publicly available for the early April seasonal hurricane forecasts) called for an El Niño (defined by NOAA to be a Niño-3.4 ≥0.5°C) event by August–October (Fig. 4), and the official March 2017 forecast from the Climate Prediction Center (CPC)/International Research Institute (IRI) also indicated a greater than 50% chance of El Niño conditions by August–October (figure not shown). This El Niño did

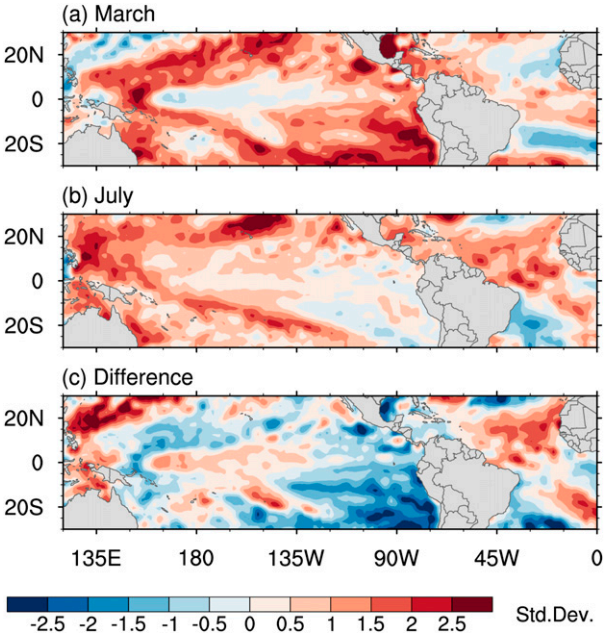

FIG. 3. Observed standardized SST anomalies in (a) March 2017, (b) July 2017, and (c) anomalous standardized SST change from March to July 2017.

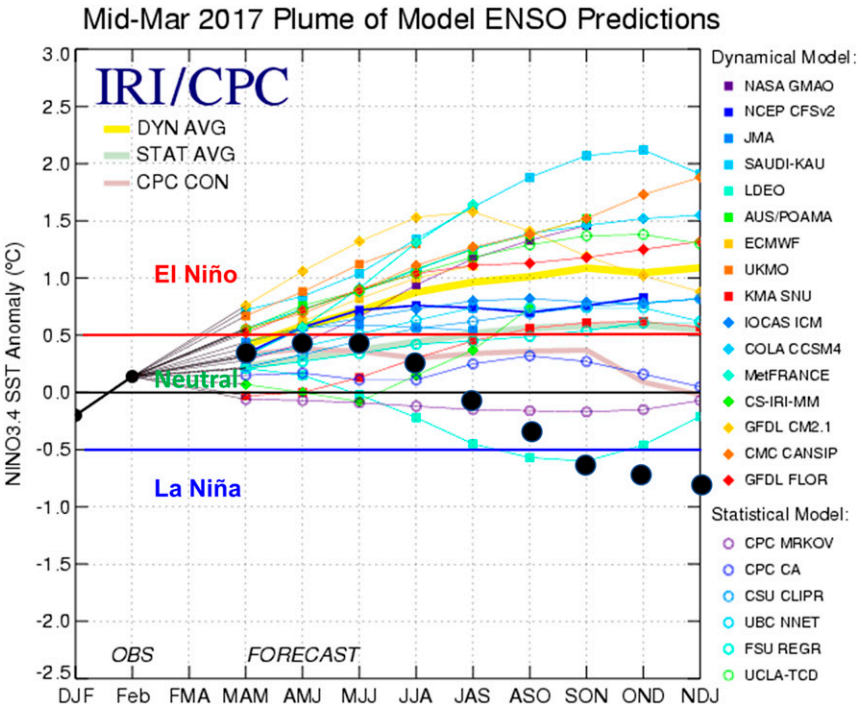

FIG. 4. Mid-March 2017 ENSO prediction plume from 16 dynamical models and six statistical models. The black dots represent observed values for each 3-month period. (Adapted from figure available at https://iri.columbia.edu/our-expertise/climate/forecasts/enso/2017-March-quick-look/.)

not develop as anticipated by many of the forecast models. Figures 3b and 3c show the standardized (1982–2010 base period) SST anomalies in July 2017 and the July minus March 2017 standardized SST anomaly change, respectively. ENSO remained in neutral conditions, with anomalous warming occurring in the central Pacific and anomalous cooling occurring in the eastern Pacific from March to July. By the end of July, it was clear that El Niño was not going to develop as predicted earlier and was one of the primary reasons why seasonal forecasts increased from June to August.

Following a westerly wind burst in late April/early May that reinforced the expectation of El Niño, the trade winds remained strong across the eastern and central tropical Pacific from May through July (Fig. 5). Consequently, there was very little oceanic Kelvin wave activity during the spring and early summer of 2017. As such, equatorial oceanic heat content in the eastern and central Pacific (180°–100°W) peaked in May 2017 and anomalously cooled over the next several months (figure not shown). Niño-3.4 SST anomalies increased from March to July, but the Pacific Walker circulation index remained strongly positive throughout the spring and summer (Fig. 6), indicating an upper-level wind environment that would likely be quite conducive for an active Atlantic hurricane season. Although the Pacific Walker circulation index and Niño-3.4 SST anomalies are strongly correlated (r = 0.64 for August–October-averaged values), this correlation value indicates that approximately 60% of the variance in the August–October Pacific Walker circulation index is explained by phenomena other than the Niño-3.4 index over the period from 1982 to 2017.

c. *Tropical Atlantic SST changes from March to July*

Portions of the eastern and central tropical Atlantic had below-normal SSTs in March (Fig. 3a). A cooler-than-normal tropical Atlantic is generally unfavorable for Atlantic hurricane activity because it creates less-conducive dynamic and thermodynamic conditions in the tropical Atlantic (Klotzbach 2014, and references therein). The early April seasonal outlook from CSU explicitly noted the anomalously cool eastern and central tropical Atlantic as one of the reasons for its slightly below-normal initial outlook for the 2017 season (Klotzbach and Bell 2017). However, the correlation between March SST anomalies in the tropical Atlantic and August–October SST anomalies in the tropical Atlantic is ~0.5 (figure not shown), indicating that there is a considerable amount of

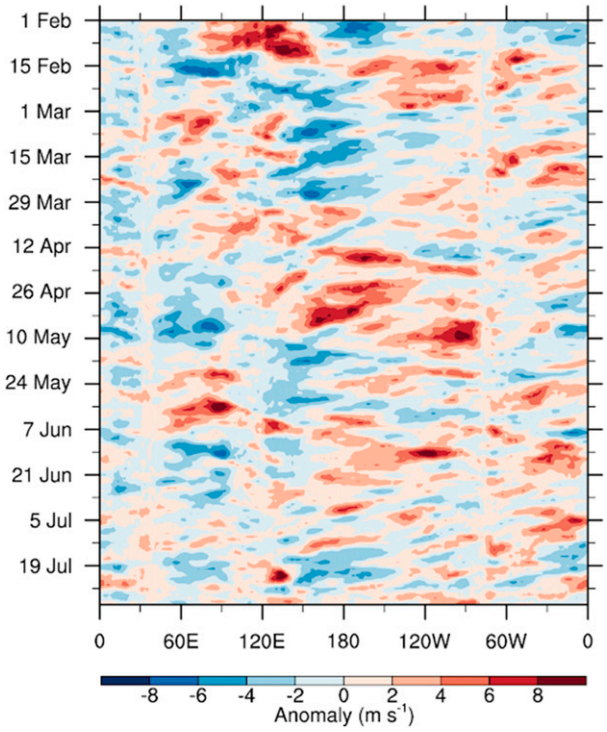

FIG. 5. The 850-hPa zonal wind anomalies averaged from 5°S–5°N from February through July 2017.

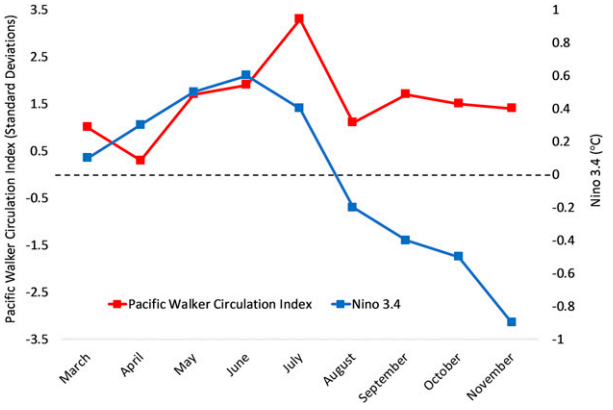

FIG. 6. Monthly values of the standardized Pacific Walker circulation index and the Niño-3.4 index (°C) from March through November 2017. The black dotted line denotes 0 standard deviations for the Pacific Walker circulation index and a 0.0° temperature anomaly for Niño-3.4.

variability not explained by simple persistence of tropical Atlantic SSTs from March through August–October. In 2017, the conditions changed rapidly from spring to summer in the tropical Atlantic.

Figures 3b and 3c show that the tropical Atlantic warmed anomalously from March to July, with unusually high SSTs present across the Atlantic main development region by July. SST anomalies averaged across the central and eastern tropical Atlantic (10°–20°N, 60°–20°W) increased from −0.1°C in March to +0.7°C in July. From April to July, anomalously low pressure dominated the subtropical Atlantic (Fig. 7a), thereby driving weaker trade winds (anomalously westerly) across most of the main development region (Fig. 7b). Weaker trade winds are associated with reduced evaporation, mixing, and upwelling, all favoring anomalous SST increases (Kossin and Vimont 2007). Anomalously high SSTs, weak trade winds, enhanced low-level vorticity, and reduced levels of vertical wind shear are all characteristics of a positive phase of the Atlantic meridional mode (Vimont and Kossin 2007; Kossin and Vimont 2007; Patricola et al. 2014). These favorable main development region conditions typically lead to more active Atlantic hurricane seasons, especially when combined with La Niña conditions (Patricola et al. 2014). The Atlantic meridional mode became more conducive for the Atlantic hurricane season from March to July, with the index increasing from −0.2 standard deviations in March to +1.1 standard deviations by July.

5. Analysis of August–October 2017 environmental conditions

In the next few subsections, we analyze large-scale environmental conditions during the peak months of the 2017 Atlantic hurricane season from August through October.

a. Main development region SSTs

As noted in the previous section, the main development region was much warmer than normal by the peak of the hurricane season (Fig. 8). During the extremely active month of September, main development region SSTs averaged ~0.6°C above the 1982–2010 average and were the highest on record (since 1982). Anomalously high SSTs can provide more latent and sensible heat for hurricanes to tap, thereby increasing the maximum potential intensity that these storms can reach (Emanuel 1988). Hurricanes Harvey, Irma, Jose, and Maria all generally formed over areas with anomalously high SSTs.

As Irma, Jose, and Maria tracked farther westward into the central Atlantic, SST anomalies were generally lower (although still above normal), but actual SSTs increase from east to west across the tropical Atlantic. Consequently, the SSTs that these TCs encountered as they entered the central and western Atlantic were high enough (~28°–29°C) to support major hurricane intensity.

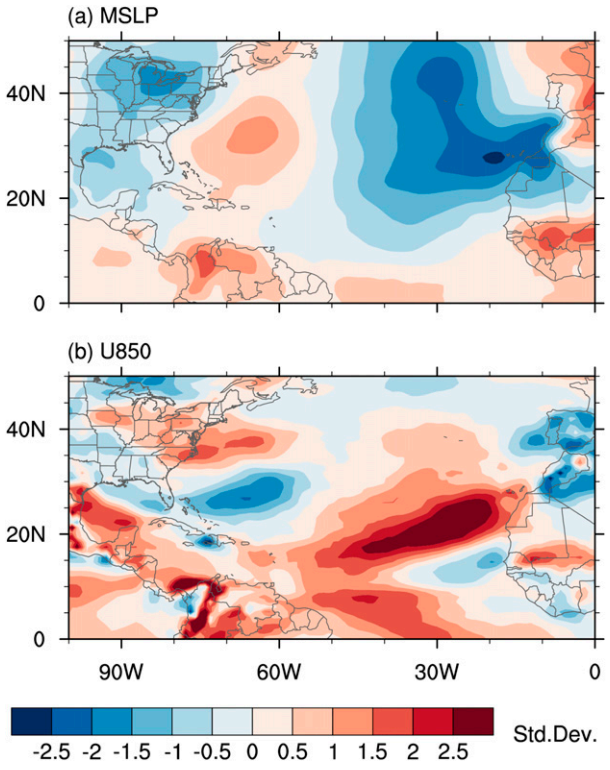

FIG. 7. (a) April–July 2017 averaged standardized SLP anomalies across the tropical and subtropical Atlantic and (b) April–July 2017 averaged standardized 850-hPa zonal wind anomalies across the tropical and subtropical Atlantic.

As would be expected, given the anomalously high SSTs across the tropical Atlantic, the Atlantic meridional mode was also positive in August, September, and October. The Atlantic meridional mode was +0.9 in August, +1.2 in September, and +0.8 in October. The September 2017 value of the Atlantic meridional mode was the fourth-highest September value since 1982.

b. *Main development region vertical wind shear*

Vertical wind shear across the Caribbean and western tropical Atlantic was generally weaker than normal during the peak of the Atlantic hurricane season in 2017, while vertical wind shear was somewhat stronger than normal in the eastern tropical Atlantic in September and October (Fig. 9). Figure 10 displays weekly maps of vertical wind shear and illustrates the climatological increase in shear late in the year. Large portions of the tropical Atlantic experienced shears less than $10\,m\,s^{-1}$ (dashed lines) in August, which are generally considered favorable shear values for TCs (e.g., Gray 1968). This area of less than $10\,m\,s^{-1}$ of shear gradually waned and gave way to large swaths of shear over $15\,m\,s^{-1}$ (solid lines) by late October, which prohibits most TC development. September was the transitional month between these extremes. The shear remained weak ($<10\,m\,s^{-1}$) over the main development region for most of the month, especially in the central tropical Atlantic (10°–25°N, 75°–55°W), where Irma, Jose, and Maria reached their maximum intensities (Figs. 10, 11). Vertical wind shear was generally much weaker throughout most of the season in the central tropical Atlantic, with values often less than one standard deviation weaker than normal from late August through mid-September (Fig. 11). While shear was anomalously low in the central tropical Atlantic in early October, analysis of satellite imagery indicated no organized disturbances tracking into the region during that time.

Aside from SSTs, vertical wind shear is often viewed as the dominant environmental factor for seasonal TC forecasting (e.g., Gray 1984; Klotzbach 2007; Camargo et al. 2007; Klotzbach et al. 2017). Collins and Roache (2011) note the importance of examining month-to-month variations, which are neglected by standard analysis methods of taking a 3- or 4-month seasonal mean to characterize the atmospheric conditions over the season. Indeed, the monthly shear anomalies from 2017 (Fig. 9) illustrate the complexity of this relationship. Shear was generally near climatological levels across most of the basin during August, consistent with the climatological TC activity. The shear was somewhat decreased around the Yucatan, where Hurricanes Franklin and Harvey both intensified. Contrary to what would be expected with the extreme activity in September, vertical wind shear was elevated over portions of the basin. This paradox can be explained in part by the stronger negative anomalies near Hispaniola and the Lesser Antilles (Fig. 9). These anomalies provided a pocket of favorable conditions within which Irma, Jose, and Maria reached their maximum intensity. The season ended in October with positive shear anomalies dominating most of the main development region (Fig. 9).

c. *ENSO*

The 2017 hurricane season started off with ENSO neutral conditions with anomalous cooling of the tropical eastern and central Pacific SSTs occurring during the season (Fig. 6). By early November, NOAA declared that a weak La Niña event was underway. The Niño-3.4 index (defined as SST anomalies from 5°S–5°N, 170°–120°W) was +0.6°C in June and cooled to −0.9°C by November. Given the borderline weak La Niña conditions that predominated during the peak of the Atlantic hurricane season, vertical wind shear was generally reduced across the Caribbean and central tropical Atlantic (section 5b), especially during August and September when there was limited MJO

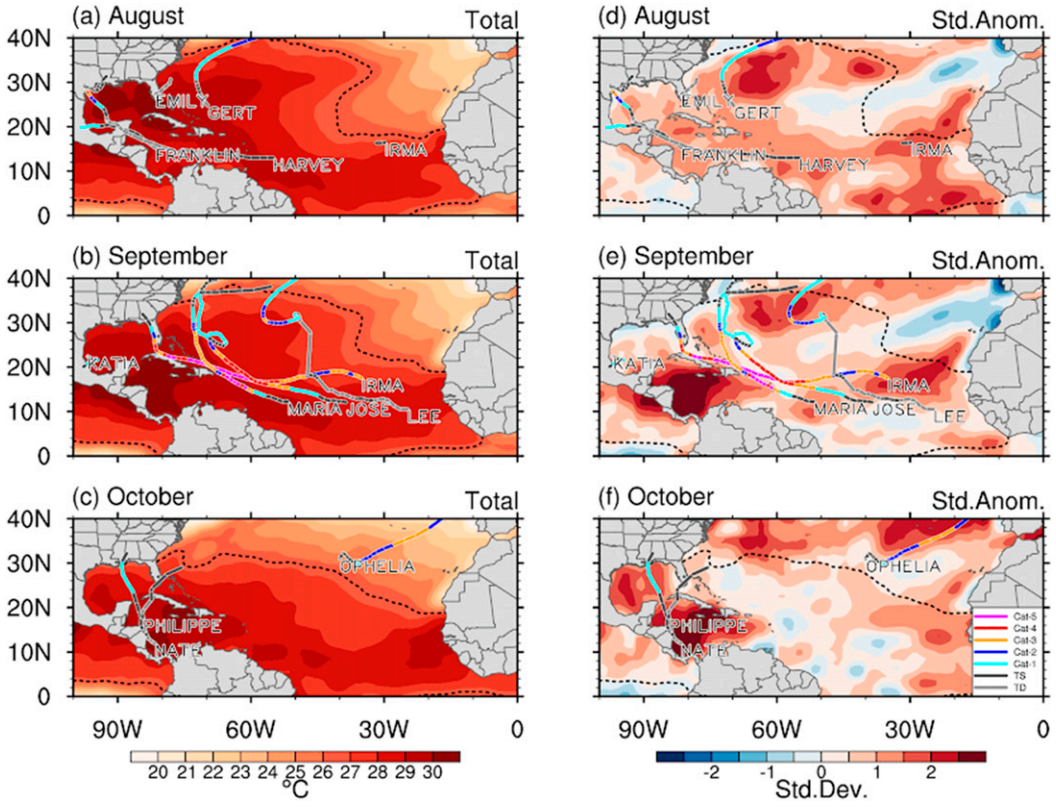

FIG. 8. (left) Observed SSTs and (right) anomalous standardized SSTs during August–October 2017. Tracks of named storms are also plotted. The base period for which anomalies are calculated is 1982–2010. The dotted black line represents the 26.5°C isotherm.

forcing (section 5d). Figure 12 shows Hovmöllers of OLR and zonal wind shear to identify variations in the Walker circulation associated with ENSO and the MJO. The Walker circulation was generally quite strong (Fig. 6), with positive OLR anomalies in the central tropical Pacific (indicating suppressed convection) and negative OLR anomalies in the western tropical Pacific (indicating enhanced convection) (Fig. 12a). These vertical circulations manifest themselves as enhanced easterly shear over the Indian Ocean and westerly shear over much of the Pacific (Fig. 12b). This increase in strength of the Walker circulation and associated reduction in Caribbean/western Atlantic wind shear (Figs. 9a,b) is consistent with prior research documenting the influence of ENSO on large-scale tropical Atlantic/Caribbean conditions (e.g., Gray 1984, and many others).

d. *Madden–Julian oscillation*

Given the background state of weak La Niña conditions and anomalously warm conditions in the Caribbean, the enhanced Atlantic TC activity was expected to continue into October/November (Klotzbach 2011b). Tropical intraseasonal variability driven by the MJO was very weak during August and September (Fig. 13). However, the MJO amplified early in October and progressed through phases 4–7 over the course of the month. These phases of the MJO tend to be unfavorable for Atlantic TC formation in the tropics (Mo 2000; Klotzbach 2010). Anomalously strong vertical wind shear progressed across the Caribbean and tropical Atlantic during October (Fig. 12b, right). As such, vertical wind shear anomalies during October were quite strong throughout most of the tropical Atlantic and extended into the eastern Caribbean (Fig. 9c), inhibiting TC development in the deep tropics.

e. *Steering currents*

Whereas Atlantic hurricane activity was near its long-term average during the period from 2006 to 2016, the midlatitude steering flow tended to favor recurvature of TCs east of the U.S. mainland (Truchelut and Staehling 2017). This was not the case in 2017. Figure 14 shows weekly standardized 500-hPa winds and geopotential heights from early August to late October, which are often used as proxies for steering flow. During the

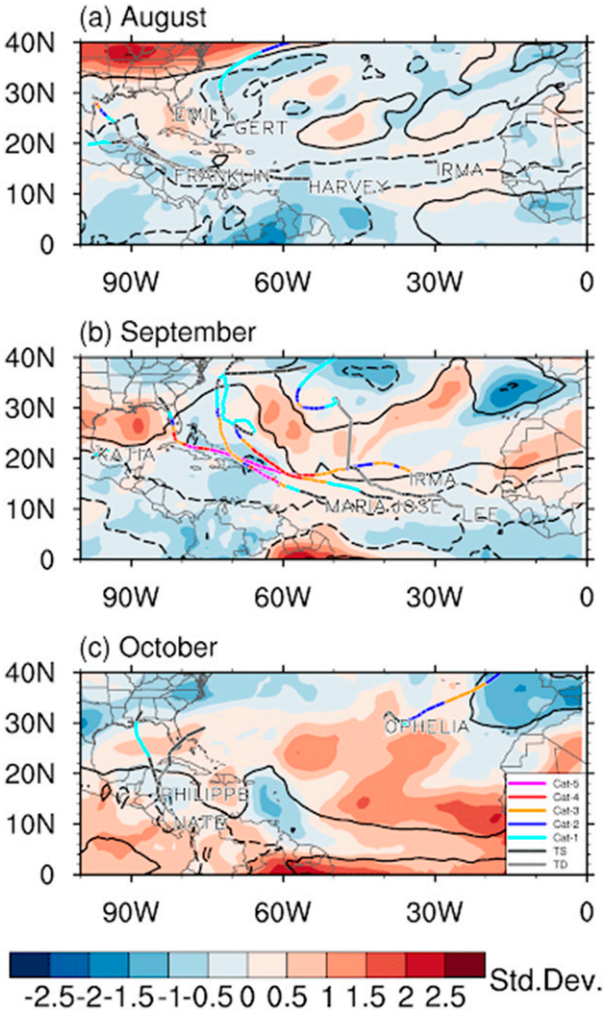

FIG. 9. Standardized vertical wind shear (200 minus 850 hPa) anomalies across the tropical and subtropical Atlantic in (a) August, (b) September, and (c) October 2017. Tracks of named storms are also displayed.

extremely active month of September, the subtropical high was generally stronger than normal in the western Atlantic near 70°W (Figs. 14e–h). In addition, an anomalous low pressure area tended to dominate near 30°–35°N, 60°–50°W. The anomalous counterclockwise circulation around this low pressure area prevented early recurvature of Irma, Jose, and Maria. Throughout Irma's tenure as a named storm (Figs. 14e,f), the subtropical high was strong and imparted a west-southwestward component to Irma's track for several days during its lifetime. By the time it turned north, it was too far west to avoid making landfall in Florida. However, the western extent of the subtropical high started to erode later in September (Figs. 14g–i), which likely contributed to Jose and Maria's recurvature east of the U.S. mainland.

6. Comparison of 2017 with recent active Atlantic hurricane seasons

Although the 2017 Atlantic hurricane season was a very active one, other recent hurricane seasons have had levels of activity comparable to what was experienced in 2017. In this section, we examine large-scale environmental conditions in 2017, compared with the five seasons that have generated the most Atlantic ACE since 1982: 1995, 1998, 1999, 2004, and 2005. We have limited our analysis to active Atlantic hurricane seasons over the past ~35 years due to availability of the atmosphere/ocean products used for analysis in this manuscript. We also evaluate August–October SST and vertical wind shear in the main development region for all Atlantic hurricane seasons since 1982 and see how these large-scale conditions correlate with August, September, and October ACE as well as total August–October ACE. In addition, SST and vertical wind shear characterizing the most active 30-day period in 2017 is compared with other active 30-day periods since 1982. In several cases, we will examine the annual rankings of these metrics from 1982 to 2017. These will be ranked from 1, indicating the most favorable for TCs (highest SST or weakest shear), to 36, indicating the least favorable for TCs (lowest SST or strongest shear).

a. Seasonal ACE distribution in active Atlantic hurricane seasons since 1982

Figure 15 displays daily Atlantic ACE (with a 15-day smoother applied) for 1995, 1998, 1999, 2004, 2005, 2017, and the 1981–2010 average. This figure demonstrates that active Atlantic hurricane seasons can have very different ACE distributions. For example, both 2004 and 2017 were characterized by extremely active Septembers, while 2005 had a much longer, drawn-out hurricane season. The 2004 and 2017 seasons had activity drop off rapidly in early October. In 2004, this was likely due to the strengthening of El Niño conditions and associated increases in vertical wind shear (not shown), while in 2017, the strengthening of the MJO in convectively unfavorable phases for Atlantic hurricane activity likely suppressed late-season activity (section 5d). The 2005 season had an extremely active July due to a combination of near-record-high SST anomalies across the main development region and convectively favorable phases of the MJO (e.g., phases 1 and 2) during the first half of July when Dennis and Emily formed—both of which generated large amounts of ACE.

b. Large-scale climate mode characteristics of active Atlantic hurricane seasons since 1982

Two climate modes known to impact Atlantic hurricane activity on a seasonal level are the Atlantic

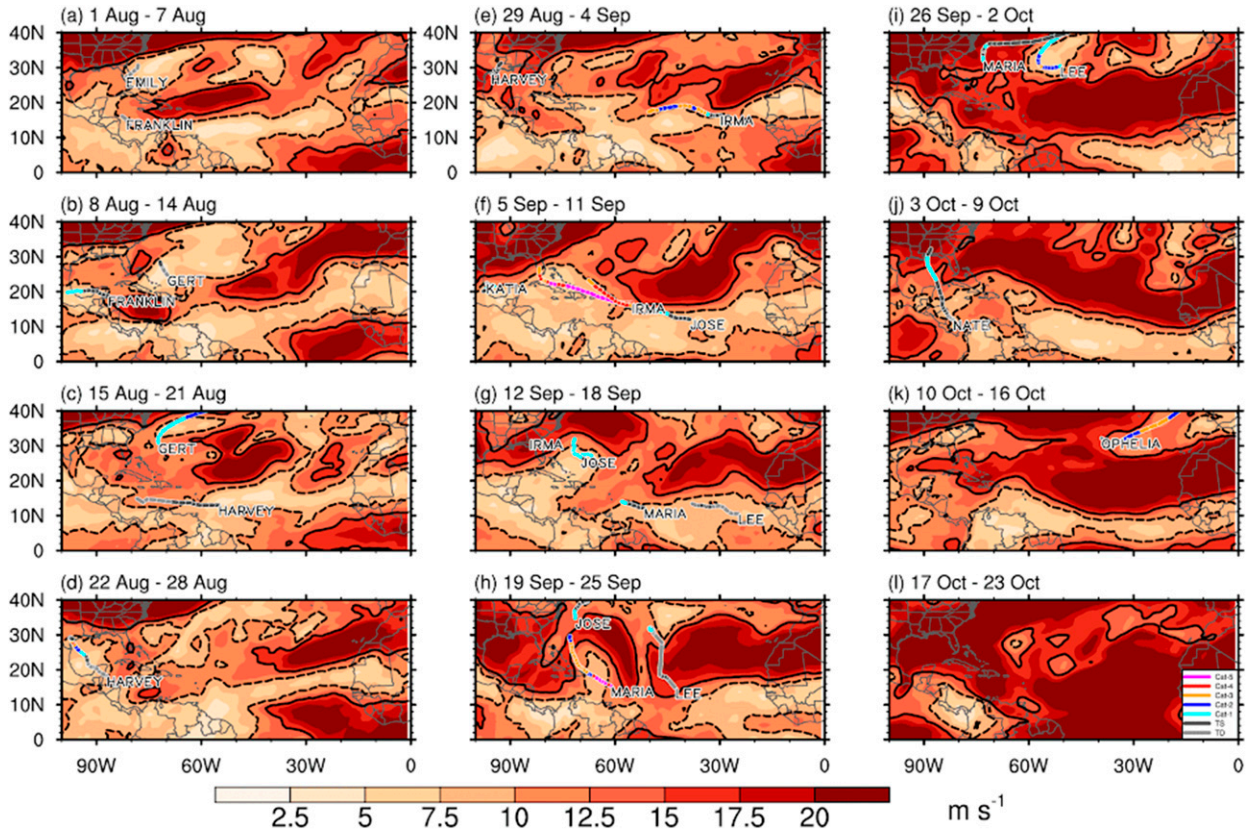

FIG. 10. Observed weekly values of vertical wind shear (200 minus 850 hPa) from 1 Aug through 23 Oct 2017. Tracks of named storms during each week are also plotted. The black dashed line denotes the 10 m s^{-1} contour, and the black solid line denotes the 15 m s^{-1} contour.

meridional mode and ENSO. Table 2 displays August–October-averaged values of these oscillations, with ENSO represented by Niño-3.4, for the six most active Atlantic hurricane seasons based on ACE since 1982: 1995, 1998, 1999, 2004, 2005, and 2017. All six hurricane seasons were characterized by positive values of the Atlantic meridional mode. Five out of the six seasons also had neutral-to-La Niña conditions, with the exception being 2004, which had weak El Niño conditions based on the CPC definition (http://origin.cpc.ncep.noaa.gov/products/analysis_monitoring/ensostuff/ONI_v5.php). However, as was noted earlier, September 2004 (the most active Atlantic calendar month for ACE prior to September 2017) had a Pacific Walker circulation index that was the eighth-highest September value from 1982 to 2017, indicating that the atmospheric circulation in the Atlantic was much more conducive than would have been expected from examining SST anomalies alone. The abrupt end to the 2004 Atlantic hurricane season (as seen in Fig. 15) is consistent with the marked increase in vertical wind shear typically observed in the Caribbean and western Atlantic in October/November of El Niño seasons (Klotzbach 2011b). The October 2004 Pacific Walker circulation index plummeted to the 12th-lowest October value from 1982 to 2017.

c. *Main development region SST characteristics of Atlantic hurricane seasons since 1982*

Figure 16a displays a scatterplot between August–October ACE and August–October-averaged SST from 1982 to 2017 for the peak of the Atlantic hurricane season from August through October, while individual monthly correlations are displayed in Table 3. Although there is little correlation between one season's ACE and the next ($r = 0.29$), there is higher autocorrelation between one season's SST and the next. We adjust for the actual estimated degrees of freedom for each time series using the methodology outlined by Leith (1973). A two-tailed Student's t test is used for statistical significance testing.

All three peak season months (August, September, and October) have similar correlations between SST and monthly ACE of between 0.42 and 0.51 (Table 3). The correlation increases to 0.59 for the August–October average. August–October SST in the main development region is a strong (significant at the 1% level) predictor

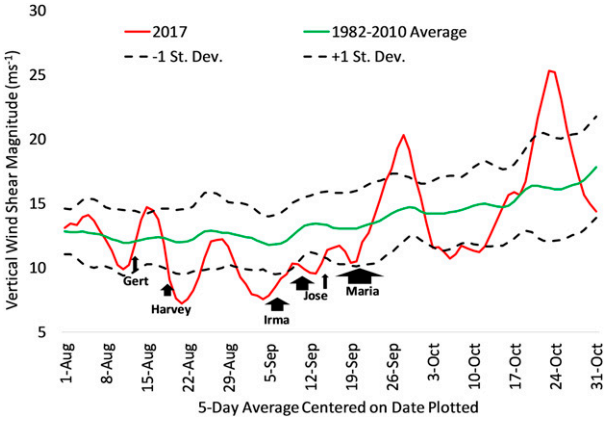

FIG. 11. Observed daily (with a 5-day smoother applied) vertical wind shear (200 minus 850 hPa) across the central tropical Atlantic (10°–25°N, 75°–55°W) from August to October. The width of the arrow for a storm is proportional to the length of the time that the storm spent in the central tropical Atlantic. Note that Jose entered the central tropical Atlantic twice due its anomalous looping characteristics.

of August–October ACE. However, the correlation of 0.59 indicates that considerable variance (e.g., ~65%) is explained by other factors such as vertical wind shear, which will be examined in the next subsection.

Figure 17a displays ranks of August-, September-, and October-averaged main development region SST for 1995, 1998, 1999, 2004, 2005, and 2017, compared with all seasons since 1982. Five out of the top six seasons had warmer-than-median (rank <16) main development region SSTs throughout the peak of the Atlantic hurricane season. As noted earlier, September 2017 had the warmest main development region on record, and the month generated the most ACE in an Atlantic calendar month on record.

d. Main development region vertical wind shear (200 minus 850 hPa) characteristics of Atlantic hurricane seasons since 1982

Figure 16b displays a scatterplot of ranked August–October ACE with ranked August–October-averaged main development region vertical wind shear. September vertical wind shear has the strongest correlation with ACE of an individual month (Table 3), while the August–October-averaged vertical wind shear correlates with August–October ACE at −0.59, which is significant at the 1% level and is the same as the correlation between August–October ACE and August–October SST. This finding is in keeping with many previous studies documenting the critical importance of vertical wind shear in determining TC formation and intensification

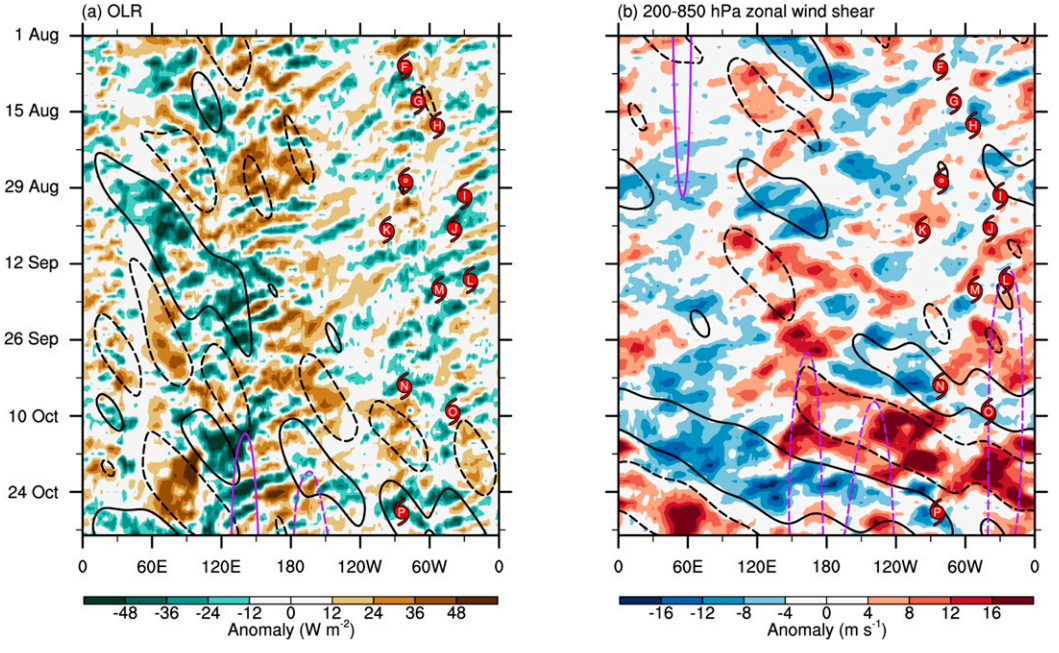

FIG. 12. (a) Hovmöller plots of OLR and (b) zonal vertical wind shear anomalies both averaged from 0° to 10°N from 1 Aug through 31 Oct. Black lines identify the MJO by filtering for eastward-propagating wavenumbers 0–9 and periods of 20–100 days following Kiladis et al. (2005). The low-frequency background is identified in purple using a 120-day low-pass filter with zonal wavenumbers 0–10, both eastward and westward. Filtered OLR anomalies are contoured at $\pm 8\ \mathrm{W\ m^{-2}}$ (positive dashed) and zonal vertical wind shear at $\pm 4\ \mathrm{m\ s^{-1}}$ (negative dashed). The letters in the red TC symbols represent the location and time when the Atlantic named storm starting with that letter formed.

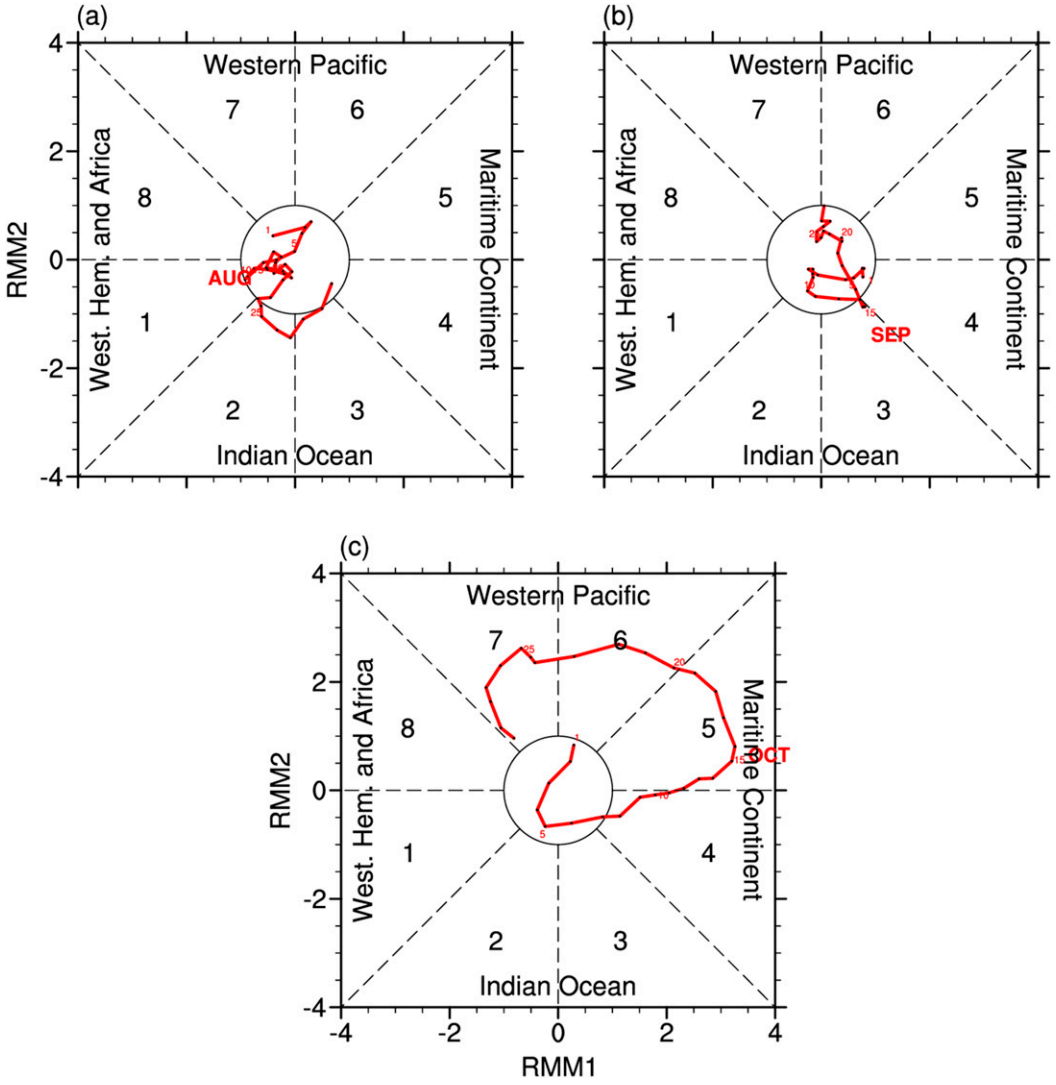

FIG. 13. MJO propagation as defined using the Wheeler and Hendon (2004) algorithm during (a) August, (b) September, and (c) October 2017.

(e.g., Gray 1968; DeMaria et al. 2001; Zheng et al. 2007; Yan et al. 2017).

In an analysis similar to section 6c, we now look at main development region ranks of vertical wind shear (200 minus 850 hPa) from August to October for the most active Atlantic hurricane seasons since 1982 (Fig. 16b). Most of these active seasons were characterized by below-normal levels of main development region vertical wind shear. Figure 16b highlights how conditions evolved over the course of the 2017 hurricane season. August 2017 had below-normal shear, and September was near normal. By October, the active MJO in convectively suppressed phases over the Atlantic (Fig. 13) helped raise shear to the fifth-highest level (31st). The resulting August–October 2017 rank of 21st is the highest seasonal shear of any of the six most active seasons since 1982. Shear was much lower than normal in the central tropical Atlantic (where Irma, Jose, and Maria all reached peak intensity) during September (Fig. 11). We also note that 1999, the season with the coolest SSTs of the most active ACE seasons since 1982, was in the top five for weakest vertical wind shear in August, September, and October. While the thermodynamic environment in 1999 may have been less conducive for an active season, it was compensated for by favorable dynamic conditions.

e. Comparison of active 30-day Atlantic ACE periods since 1982

Last, we examine how SST and vertical wind shear in the main development region compared in 2017 to other

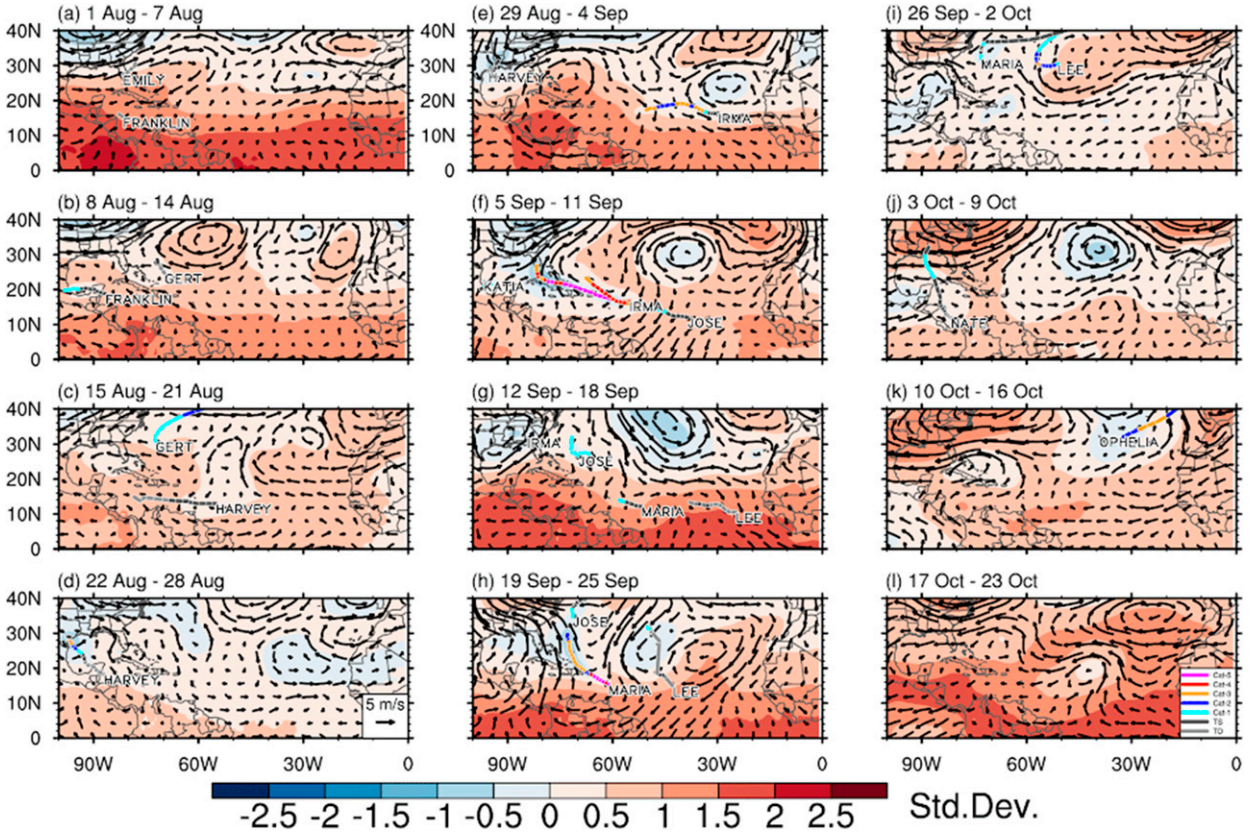

FIG. 14. Weekly 500-hPa standardized geopotential height anomalies and 500-hPa vector winds across the tropical and subtropical North Atlantic from 1 Aug through 23 Oct 2017. Tracks of named storms are plotted.

30-day active periods since 1982. Table 4 displays the most active 30-day period in 2017, compared with the five other most active 30-day periods for ACE since 1982. Only one active period per season was selected. Table 4 also shows the 30-day-average 24 August–22 September ACE, SST, and vertical wind shear, which is the average start date of the six active 30-day periods being examined here.

All of these active periods had SSTs that were at least 0.7 standard deviations warmer than normal. Vertical wind shear was also at least 0.5 standard deviations below normal for each of the 30-day periods. The most active 30-day period in 2017 was characterized by the second-warmest SST anomalies experienced during that 30-day period. Vertical wind shear was slightly weaker than normal, but still had the smallest standardized anomaly reduction from climatology of any of the six active 30-day periods being investigated. This serves to illustrate that basinwide-averaged quantities, while useful, do not necessarily tell the whole story for why individual months or seasons have as much hurricane activity as they do.

7. Discussion and summary

a. Discussion of Atlantic hurricane seasonal and subseasonal outlooks

The extremely active 2017 Atlantic hurricane season was not well anticipated by most seasonal forecast models. Even though outlooks issued in early August predicted an above-average Atlantic hurricane season, these predictions still called for much less activity than was observed (Table 1). Although ENSO SST indices indicated a neutral-to-El Niño state in June/July (Fig. 6), the Pacific Walker circulation index was at its strongest levels on record (since 1982). Both the Pacific Walker circulation index and Niño-3.4 have similar August–October correlation magnitudes with seasonal Atlantic ACE ($r = 0.46$ and $r = -0.45$, respectively), but the Pacific Walker circulation index could be a better indicator of the impacts of ENSO in the Atlantic basin than SST indices by themselves. Another recent example of this is September 2004, which was the most active ACE Atlantic calendar month on record prior to

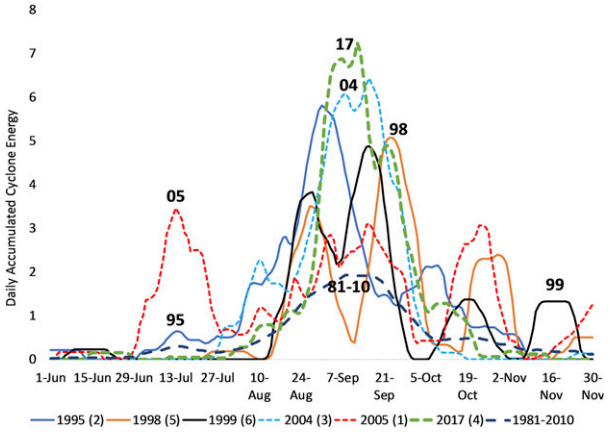

FIG. 15. Daily Atlantic ACE (with a 15-day average applied) for 1995, 1998, 1999, 2004, 2005, and 2017—the six most active Atlantic hurricanes seasons based on ACE since 1982. The 15-day average is centered on the date plotted. Seasons since 2000 are dotted for ease of viewing. The numbers in parentheses in the legend are the overall rank for seasonal ACE since 1982. Also plotted is the 1981–2010 average.

September 2017. The Niño-3.4 index was +0.8°C that month, indicating a weak El Niño event. During that same month, however, the Pacific Walker circulation index was +1.0 standard deviations, indicating a much more conducive atmospheric circulation environment for Atlantic hurricanes.

From a predictive perspective, the June/July Pacific Walker circulation index and June/July Niño-3.4 could be examined in tandem for potential increased skill for early August seasonal outlooks. For example, in 2012, the June/July-averaged Niño-3.4 index was +0.4°C, and many forecast models indicated a potential El Niño developing (figure not shown). However, the June/July-averaged Pacific Walker circulation index was the third strongest on record. The anomalously strong Pacific Walker circulation and associated anomalously strong tropical Pacific trades inhibited El Niño development that year. Consequently, the ASO-averaged Walker circulation index in 2012 was the eighth-most positive on record, and the 2012 Atlantic hurricane season was very active with 10 hurricanes developing. In the future, it may be helpful for seasonal forecast groups to pay close attention to the Walker circulation index when monitoring ENSO conditions.

TABLE 2. Aug–Oct averaged Atlantic meridional mode and ENSO (as measured by Niño-3.4) values for the six most active Atlantic hurricane seasons since 1982: 1995, 1998, 1999, 2004, 2005, and 2017. Ranks compared with all years since 1982 are provided in parentheses, where 1 represents the strongest Atlantic meridional mode, the coldest Niño-3.4, and the highest seasonal ACE.

Year	Atlantic meridional mode (std dev)	Niño-3.4 (°C)	Seasonal ACE
1995	+1.2 (5)	−0.8 (7)	227 (2)
1998	+0.8 (10)	−1.3 (3)	182 (5)
1999	+0.6 (16)	−1.1 (4)	177 (6)
2004	+1.4 (3)	+0.7 (30)	227 (3)
2005	+1.4 (2)	0.0 (20)	245 (1)
2017	+1.0 (7)	−0.3 (15)	225 (4)

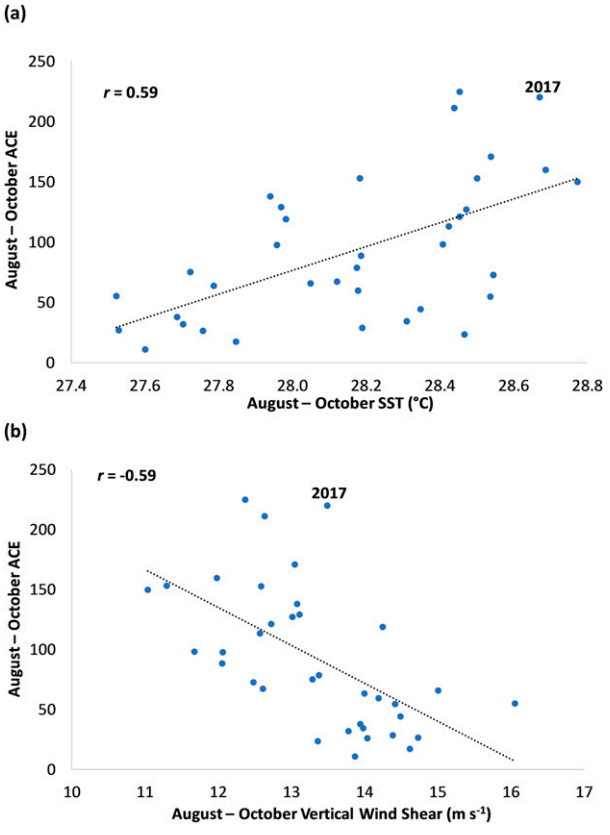

FIG. 16. (a) Scatterplot of August–October averaged SST vs August–October ACE and (b) scatterplot of August–October averaged vertical wind shear vs August–October ACE. Values for 2017 are highlighted. Correlations between SST and ACE and vertical wind shear and ACE are also plotted. The black dotted lines represent the regression line for each relationship.

The MJO played an important role in dampening late-season Atlantic hurricane activity (Fig. 13). The increase in strength of the MJO in convectively unfavorable phases for Atlantic TC activity counteracted the typical response of heightened Atlantic hurricane activity in October/November of seasons with anomalously warm SSTs in the Caribbean and anomalously cool SSTs in the eastern and central tropical Pacific (Klotzbach 2011b). Strong subseasonal variability driven by the MJO can counteract SST forcing, as shown by Klotzbach and Oliver (2015).

TABLE 3. Aug, Sep, and Oct correlations between SST and ACE, and vertical wind shear and ACE, respectively. Correlations that are significant at the 5% level using a two-tailed Student's *t* test are highlighted in boldface font.

Geophysical parameter	Aug ACE	Sep ACE	Oct ACE
SST	**0.45**	**0.51**	0.42
Vertical wind shear	**−0.43**	**−0.53**	−0.22

b. Summary

The 2017 Atlantic hurricane season was an extremely active one, with 17 named storms, 10 hurricanes, and 6 major hurricanes occurring (Fig. 1). September was particularly noteworthy. It was the most active Atlantic calendar month on record for named storm days, hurricane days, major hurricane days, and ACE. The season also had four hurricanes retired by the WMO (Harvey, Irma, Maria, and Nate). These hurricanes caused death and destruction for portions of the Gulf Coast and southeastern United States as well as Cuba, Puerto Rico, Central America, and many other islands in the Caribbean.

Environmental conditions were conducive for an active season, with anomalously warm SSTs in the tropical Atlantic and neutral-to-La Niña conditions in the tropical Pacific (Fig. 3). The enhanced Pacific Walker circulation drove reduced vertical wind shear in the central tropical Atlantic and Caribbean, especially from late August to late September (Figs. 9–11). The reduced vertical wind shear anomalies were strongest in the central tropical Atlantic (Fig. 11), where Irma, Jose, and Maria all reached their maximum intensities during a record-breaking September. An anomalously strong high pressure system in the subtropical western Atlantic drove TCs farther west, toward the Caribbean and continental United States, compared to the previous 11 years (2006–16; Fig. 14).

We examined the other most active hurricane seasons in recent decades (1982–2017). Some years had levels of activity comparable to what was experienced in 2017, but the ACE distributions during each of these seasons were different (Fig. 15). The 2017 season had the most pronounced peak activity. We also investigated the state of the Atlantic meridional mode and ENSO for the six most active Atlantic hurricane seasons. All six of the most active hurricane seasons were characterized by positive values of the Atlantic meridional mode, and five of them also had neutral-to-La Niña conditions (Table 2).

We looked at correlations of main development region SST and vertical wind shear with ACE during the peak of the Atlantic hurricane season from August to October (Fig. 16). Warmer SSTs and reduced vertical wind shear tend to be associated with more active Atlantic hurricane seasons. Many studies (e.g., Saunders et al. 2017, and references therein) have shown that large-scale quantities such as ENSO and main development region–averaged SST or surface pressure are correlated with active seasons. However, it should also be stressed that what the TC responds to is the local-scale conditions in which the TC is embedded. Ranking environmental conditions for all seasons showed that five out of the six most active seasons had

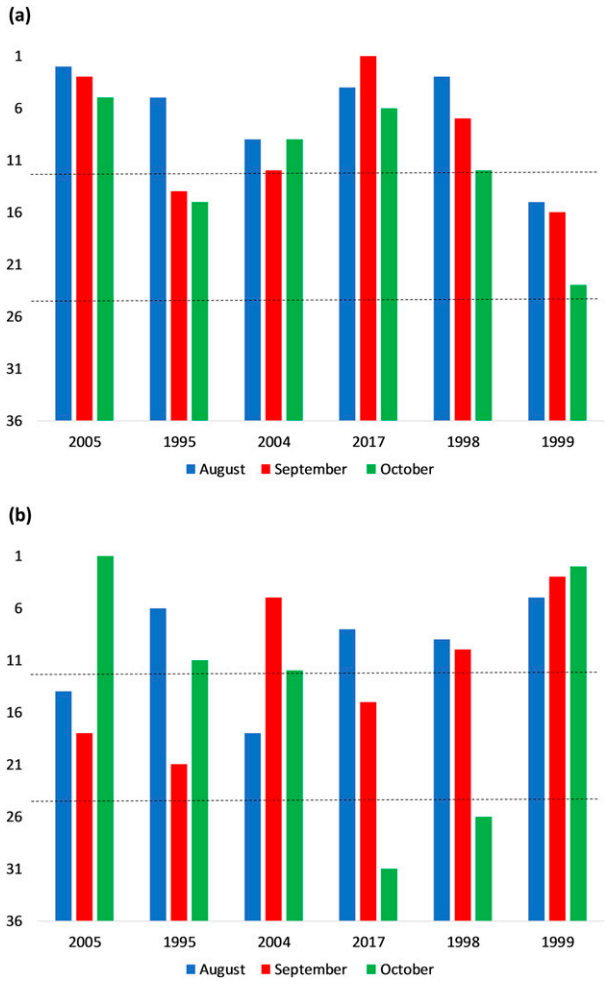

FIG. 17. (a) August, September, and October monthly ranks of SST and (b) August, September, and October monthly ranks of vertical wind shear in the six most active Atlantic ACE seasons since 1982. A rank of 1 indicates conditions that are most conducive for hurricanes (e.g., highest SSTs and lowest vertical wind shear). Years are displayed from left to right from the year with the most seasonal ACE (2005) to the year with the sixth-most ACE (1999). Black lines indicate year rank terciles (e.g., years 1–12 represent the upper tercile, years 13–24 represent the middle tercile, and years 25–36 represent the lower tercile).

TABLE 4. SST and vertical wind shear averaged over the main development region for the most active 30-day periods since 1982. The standardized value compared with the 1982–2010 base period for the 30-day period is listed in parentheses. Also displayed is the average 24 Aug–22 Sep value—the average of the six most active 30-day periods displayed.

30-day period	SST (°C)	Vertical wind shear ($m\,s^{-1}$)	ACE
31 Aug–29 Sep 2017	28.7 (+1.8)	11.7 (−0.5)	175 (+3.4)
28 Aug–26 Sep 2004	28.2 (+0.8)	10.3 (−1.3)	174 (+3.0)
11 Aug–9 Sep 1995	28.1 (+0.8)	10.5 (−0.7)	127 (+2.9)
22 Aug–20 Sep 1999	28.2 (+0.8)	10.4 (−1.2)	121 (+1.7)
23 Aug–21 Sep 2010	28.7 (+2.0)	9.5 (−2.0)	118 (+1.6)
30 Aug–28 Sep 2003	28.2 (+0.7)	11.4 (−0.7)	115 (+1.7)
24 Aug–22 Sep average (1982–2010)	27.9	11.9	50

warmer-than-average main development region SSTs and below-normal levels of vertical wind shear throughout the peak of the Atlantic hurricane season (Fig. 17). September 2017 was the most active Atlantic calendar month on record, and although SST and vertical shear were conducive for an active month, they were not necessarily more favorable than other active months of the past (Table 4). Other conditions besides SSTs and vertical shear are important for active TC periods, and understanding which conditions are most important will be critical in anticipating future extremely active hurricane periods.

The 2017 Atlantic hurricane season was one of the most active and damaging on record, with total economic damage exceeding $260 billion according to NCEI. Large-scale conditions were conducive for an active season, but steering currents were also somewhat different in 2017 (Fig. 14) than those experienced during the recent drought in major hurricane landfalls for the continental United States (Hall and Hereid 2015; Hart et al. 2016; Truchelut and Staehling 2017). An enhanced subtropical high drove storms farther westward, into the eastern Caribbean and toward the continental United States. With continued growth in population and wealth along the U.S. coastline (Klotzbach et al. 2018) and in the Caribbean, future active landfalling Atlantic hurricane seasons will likely produce levels of damage comparable to or even higher than what we saw in 2017.

Acknowledgments. Klotzbach acknowledges support from a grant from the G. Unger Vetlesen Foundation. M. Bell was supported by Office of Naval Research Award N000141613033. Schreck was supported by NOAA through the Cooperative Institute for Climate and Satellites–North Carolina under Cooperative Agreement NA14NES432003. We thank John Knaff, Ron McTaggart-Cowan, two anonymous reviewers, and the editor, David Schultz, for comments that significantly improved the content of this manuscript. All climate indices, Atlantic hurricane data, and the source code used for the calculations in this paper are available at https://doi.org/10.5281/zenodo.1316916.

REFERENCES

Banzon, V., T. M. Smith, T. M. Chin, C. Liu, and W. Hankins, 2016: A long-term record of blended satellite and in situ sea-surface temperature for climate monitoring, modeling and environmental studies. *Earth Syst. Sci. Data*, **8**, 165–176, https://doi.org/10.5194/essd-8-165-2016.

Barnston, A. G., M. Chelliah, and S. B. Goldenberg, 1997: Documentation of a highly ENSO-related SST region in the equatorial Pacific: Research note. *Atmos.–Ocean*, **35**, 367–383, https://doi.org/10.1080/07055900.1997.9649597.

Bell, G. D., and Coauthors, 2000: Climate assessment for 1999. *Bull. Amer. Meteor. Soc.*, **81**, S1–S50, https://doi.org/10.1175/1520-0477(2000)81[s1:CAF]2.0.CO;2.

Beven, J. L., and R. Berg, 2018: National Hurricane Center tropical cyclone report: Hurricane Nate. NOAA/NWS Rep. AL162017, 45 pp., https://www.nhc.noaa.gov/data/tcr/AL162017_Nate.pdf.

Blake, E. S., and D. A. Zelinsky, 2018: National Hurricane Center tropical cyclone report: Hurricane Harvey. NOAA/NWS Rep. Al092017, 76 pp., https://www.nhc.noaa.gov/data/tcr/AL092017_Harvey.pdf.

Camargo, S. J., A. G. Barnston, P. J. Klotzbach, and C. W. Landsea, 2007: Seasonal tropical cyclone forecasts. *WMO Bull.*, **56**, 297–309.

Camp, J., A. A. Scaife, and J. Heming, 2018: Predictability of the 2017 North Atlantic hurricane season. *Atmos. Sci. Lett.*, **19**, e813, https://doi.org/10.1002/asl.813.

Cangialosi, J. P., A. S. Latto, and R. Berg, 2018: National Hurricane Center tropical cyclone report: Hurricane Irma. NOAA/NWS Rep. AL112017, 111 pp., https://www.nhc.noaa.gov/data/tcr/AL112017_Irma.pdf.

Collins, J. M., and D. R. Roache, 2011: The 2009 hurricane season in the eastern North Pacific basin: An analysis of environmental conditions. *Mon. Wea. Rev.*, **139**, 1673–1682, https://doi.org/10.1175/2010MWR3538.1.

——, and ——, 2017: The 2016 North Atlantic hurricane season: A season of extremes. *Geophys. Res. Lett.*, **44**, 5071–5077, https://doi.org/10.1002/2017GL073390.

DeMaria, M., J. A. Knaff, and B. H. Connell, 2001: A tropical cyclone genesis parameter for the tropical Atlantic. *Wea. Forecasting*, **16**, 219–233, https://doi.org/10.1175/1520-0434(2001)016<0219:ATCGPF>2.0.CO;2.

Emanuel, K. A., 1988: The maximum intensity of hurricanes. *J. Atmos. Sci.*, **45**, 1143–1155, https://doi.org/10.1175/1520-0469(1988)045<1143:TMIOH>2.0.CO;2.

——, 2017: Assessing the present and future probability of Hurricane Harvey's rainfall. *Proc. Nat. Acad. Sci.*, **114**, 12 681–12 684, https://doi.org/10.1073/pnas.1716222114.

Galarneau, T. J., and C. A. Davis, 2013: Diagnosing forecast error in tropical cyclone motion. *Mon. Wea. Rev.*, **141**, 405–430, https://doi.org/10.1175/MWR-D-12-00071.1.

Goldenberg, S. B., C. W. Landsea, A. M. Mestas-Nuñez, and W. M. Gray, 2001: The recent increase in Atlantic hurricane activity: Causes and implications. *Science*, **293**, 474–479, https://doi.org/10.1126/science.1060040.

Gray, W. M., 1968: Global view of the origin of tropical disturbances and storms. *Mon. Wea. Rev.*, **96**, 669–700, https://doi.org/10.1175/1520-0493(1968)096<0669:GVOTOO>2.0.CO;2.

——, 1984: Atlantic seasonal hurricane frequency. Part I: El Niño and 30 mb quasi-biennial oscillation influences. *Mon. Wea. Rev.*, **112**, 1649–1668, https://doi.org/10.1175/1520-0493(1984)112<1649:ASHFPI>2.0.CO;2.

Hall, T. R., and K. Hereid, 2015: The frequency and duration of U.S. hurricane droughts. *Geophys. Res. Lett.*, **42**, 3482–3485, https://doi.org/10.1002/2015GL063652.

Hart, R. E., D. R. Chavas, and M. P. Guishard, 2016: The arbitrary definition of the current Atlantic major hurricane landfall drought. *Bull. Amer. Meteor. Soc.*, **97**, 713–722, https://doi.org/10.1175/BAMS-D-15-00185.1.

Kiladis, G. N., K. H. Straub, and P. T. Haertel, 2005: Zonal and vertical structure of the Madden–Julian oscillation. *J. Atmos. Sci.*, **62**, 2790–2809, https://doi.org/10.1175/JAS3520.1.

Klotzbach, P. J., 2007: Recent developments in statistical prediction of seasonal Atlantic basin tropical cyclone activity. *Tellus*, **59A**, 511–518, https://doi.org/10.1111/j.1600-0870.2007.00239.x.

——, 2010: On the Madden–Julian Oscillation–Atlantic hurricane relationship. *J. Climate*, **23**, 282–293, https://doi.org/10.1175/2009JCLI2978.1.

——, 2011a: El Niño–Southern Oscillation's impact on Atlantic basin hurricanes and U.S. landfalls. *J. Climate*, **24**, 1252–1263, https://doi.org/10.1175/2010JCLI3799.1.

——, 2011b: Forecasting October–November Caribbean hurricane days. *J. Geophys. Res.*, **116**, D18117, https://doi.org/10.1029/2011JD016146.

——, 2014: Prediction of seasonal Atlantic basin accumulated cyclone energy from 1 July. *Wea. Forecasting*, **29**, 115–121, https://doi.org/10.1175/WAF-D-13-00073.1.

——, and E. C. J. Oliver, 2015: Modulation of Atlantic basin tropical cyclone activity by the Madden–Julian oscillation (MJO) from 1905 to 2011. *J. Climate*, **28**, 204–217, https://doi.org/10.1175/JCLI-D-14-00509.1.

——, and M. M. Bell, 2017: Extended range forecast of Atlantic seasonal hurricane activity and landfall strike probability for 2017. Colorado State University Dept. of Atmospheric Science Report, 41 pp., https://tropical.colostate.edu/media/sites/111/2017/04/2017-04.pdf.

——, M. A. Saunders, G. D. Bell, and E. S. Blake, 2017: Statistically-based North Atlantic seasonal hurricane outlooks. *Climate Extremes: Patterns and Mechanisms*, *Geophys. Monogr.*, Vol. 226, Amer. Geophys. Union, 315–328, https://doi.org/10.1002/9781119068020.ch19.

——, S. G. Bowen, R. Pielke Jr., and M. M. Bell, 2018: Continental U.S. hurricane landfall frequency and associated damage: Observations and future risks. *Bull. Amer. Meteor. Soc.*, **99**, 1359–1376, https://doi.org/10.1175/BAMS-D-17-0184.1.

Kossin, J. P., and D. J. Vimont, 2007: A more general framework for understanding Atlantic hurricane variability and trends. *Bull. Amer. Meteor. Soc.*, **88**, 1767–1782, https://doi.org/10.1175/BAMS-88-11-1767.

Landsea, C. W., and J. L. Franklin, 2013: Atlantic hurricane database uncertainty and presentation of a new database format. *Mon. Wea. Rev.*, **141**, 3576–3592, https://doi.org/10.1175/MWR-D-12-00254.1.

——, R. A. Pielke, A. M. Mestas-Nuñez, and J. A. Knaff, 1999: Atlantic basin hurricanes: Indices of climatic changes. *Climatic Change*, **42**, 89–129, https://doi.org/10.1023/A:1005416332322.

Leith, C. E., 1973: The standard error of time-average estimates of climate means. *J. Appl. Meteor.*, **12**, 1066–1069, https://doi.org/10.1175/1520-0450(1973)012<1066:TSEOTA>2.0.CO;2.

Lupo, A. R., T. K. Latham, T. Magill, J. V. Clark, C. J. Melick, and P. S. Market, 2008: The interannual variability of hurricane activity in the Atlantic and East Pacific regions. *Natl. Wea. Dig.*, **32**, 119–133.

Mo, K. C., 2000: The association between intraseasonal oscillations and tropical storms in the Atlantic basin. *Mon. Wea. Rev.*, **128**, 4097–4107, https://doi.org/10.1175/1520-0493(2000)129<4097:TABIOA>2.0.CO;2.

Pasch, R. J., A. B. Penny, and R. Berg, 2018: National Hurricane Center tropical cyclone report: Hurricane Maria, NOAA/NWS Rep. AL152017, 48 pp., https://www.nhc.noaa.gov/data/tcr/AL152017_Maria.pdf.

Patricola, C. M., R. Saravanan, and P. Chang, 2014: The impact of the El Niño–Southern Oscillation and Atlantic meridional mode on seasonal Atlantic tropical cyclone activity. *J. Climate*, **27**, 5311–5328, https://doi.org/10.1175/JCLI-D-13-00687.1.

Rasmusson, E. M., and T. H. Carpenter, 1982: Variations in tropical sea surface temperature and surface wind fields associated with the Southern Oscillation/El Niño. *Mon. Wea. Rev.*, **110**, 354–384, https://doi.org/10.1175/1520-0493(1982)110<0354:VITSST>2.0.CO;2.

Reynolds, R. W., N. A. Rayner, T. M. Smith, D. C. Stokes, and W. Wang, 2002: An improved in situ and satellite SST analysis for climate. *J. Climate*, **15**, 1609–1625, https://doi.org/10.1175/1520-0442(2002)015<1609:AIISAS>2.0.CO;2.

Saha, S., and Coauthors, 2010: The NCEP Climate Forecast System Reanalysis. *Bull. Amer. Meteor. Soc.*, **91**, 1015–1058, https://doi.org/10.1175/2010BAMS3001.1.

——, and Coauthors, 2014: The NCEP Climate Forecast System version 2. *J. Climate*, **27**, 2185–2208, https://doi.org/10.1175/JCLI-D-12-00823.1.

Saunders, M. A., P. J. Klotzbach, and A. S. R. Lea, 2017: Replicating annual North Atlantic hurricane activity 1878–2012 from environmental variables. *J. Geophys. Res. Atmos.*, **122**, 6284–6297, https://doi.org/10.1002/2017JD026492.

Schreck, C. J., K. R. Knapp, and J. P. Kossin, 2014: The impact of best track discrepancies on global tropical cyclone climatologies using IBTrACS. *Mon. Wea. Rev.*, **142**, 3881–3899, https://doi.org/10.1175/MWR-D-14-00021.1.

Simpson, R. H., 1974: The hurricane disaster—Potential scale. *Weatherwise*, **27**, 169–186, https://doi.org/10.1080/00431672.1974.9931702.

Tartaglione, C. A., S. R. Smith, and J. J. O'Brien, 2003: ENSO impact on hurricane landfall probabilities for the Caribbean. *J. Climate*, **16**, 2925–2931, https://doi.org/10.1175/1520-0442(2003)016<2925:EIOHLP>2.0.CO;2.

Truchelut, R. E., and E. M. Staehling, 2017: An energetic perspective on United States tropical cyclone landfall droughts. *Geophys. Res. Lett.*, **44**, 12 013–12 019, https://doi.org/10.1002/2017GL076071.

Vimont, D. J., and J. P. Kossin, 2007: The Atlantic meridional mode and hurricane activity. *Geophys. Res. Lett.*, **34**, L07709, https://doi.org/10.1029/2007GL029683.

Wang, C., 2004: ENSO, Atlantic climate variability, and the Walker and Hadley circulations. *The Hadley Circulation: Present, Past and Future*, H. F. Diaz and R. S. Bradley, Eds., Springer, 173–202, https://doi.org/10.1007/978-1-4020-2944-8_7.

Wheeler, M. C., and H. H. Hendon, 2004: An all-season real-time multivariate MJO index: Development of an index for monitoring and prediction. *Mon. Wea. Rev.*, **132**, 1917–1932, https://doi.org/10.1175/1520-0493(2004)132<1917:AARMMI>2.0.CO;2.

Yan, X., R. Zhang, and T. R. Knutson, 2017: The role of Atlantic overturning circulation in the recent decline of Atlantic major hurricane frequency. *Nat. Commun.*, **8**, 1695, https://doi.org/10.1038/s41467-017-01377-8.

Zheng, X., Y. Duan, and H. Yu, 2007: Dynamical effects of environmental vertical wind shear on tropical cyclone motion, structure, and intensity. *Meteor. Atmos. Phys.*, **97**, 207–220, https://doi.org/10.1007/s00703-006-0253-0.